BSPE 00200－371－2

톰볼로 形成에 관한 數値모델

Numerical Modeling of Tombolo Formation

1991. 7.

韓國海洋研究所

提 出 文

韓國海洋研究所長 貴下

本 報告書를 "이안제군 背後에서의 롬볼로 形成에 관한 數値모델" 과제의 最終報告書로 提出합니다.

1991年 7月

韓國海洋研究所 海洋工學研究室

研究責任者 : 徐 慶 德

要 約 文

I. 題 目

톰볼로 形成에 관한 數値모델

II. 연구 개발의 重要性 및 目的

波浪에 의한 해안 浸蝕 방지를 위해 離岸堤가 널리 사용되어 왔다. 파랑에 의해 이안제 주변에 발생된 흐름은 이안제 背後에 漂砂를 集積시켜 Salient라 불리는 융기된 해안선 형태를 만들게 된다. 간혹 이 Salient는 그 頂点이 이안제에 닿을 때까지 성장하여 톰볼로(Tombolo)를 형성하기도 하는데, 이 톰볼로의 형성을 씨뮤레이션 할 수 있는 數値모델은 거의 없다. 기존의 數値모델들은 계산된 해안선의 위치가 이안제에 이르게 되면 계산을 중단하거나, 혹은 이안제의 外海쪽으로까지 해안선이 전진하는 비현실적인 결과를 나타낸다. 본 연구에서는 불투과성 이안제 배후에서의 톰볼로의 형성 및 성장과정을 씨뮤레이션 할 수 있는 One-line 수치모델을 개발한다.

III. 연구개발의 內容 및 結果

One-line 수치모델은 해안구조물 주변에서의 해안선 변화를 예측하기 위하여 널리 사용되고 있다. 대부분의 One-line 모델들은 直交座標系를 사용하며, 좌표축 중의 하나가 해안선과 비교적 나란하게 되도록 좌표축을 설정한다. 이 경우 沿岸漂砂 및 해안선의 移動은 각각 이 좌표축에 平行 및 垂直 방향으로 일어난다고 가정한다. 그러나, 이안제 배후의 톰볼로에서와 같이 해안선이 이 좌표축과 큰 각도를 이루게 되는 경우에는 이러한 가정은 실제 현상과 크게 어긋나게 된다. 이러한 상황을 씨뮤레이션하기 위하여, 해안선의 임의점에서 해안선과 연안표사의 이동이 그 당시 그 점에서의 해안선 방향에 각각 수직 및 평행 방향으로 발생한다고 가정하여, 해안선을 따라가는 Curvilinear 좌표계를 사용한 모델들이 개발되어 왔다. 本 모델에서도 이러한 Curvilinear 좌표계가 사용된다.

해안선이 이안제의 위치까지 도달하게 되면, 그 이동이 거기서 멈추어야 한다. 그러나 이안제가 해안선의 이동을 저지시키는 현상을 포함하고 있지 않은 수치모델들은 해안선이 이안제의 외해쪽으로까지 전진하게 되는 결과를 주게 될 것이다. 본 모델은 매 계산시간 간격마다 해안선의 어느 계산점이라도 아안제를 넘어가는 것으로 계산되는지를 조사하여 만약 있으면 그 점을 이안제의 위치까지 끌어들이고 그 대신 그 점 부근의 다른 점들의 위치를 土砂의 保存법칙을 만족시키도록 다시 계산한다.

본 모델의 적용예로서 미국 Virginia주의 Chippokes 주립공원의 침식방지를 위해 건설된 이안제郡 背後에서 건설 후 9개월 동안의 해안선 변화를 모델결과와 비교하였다.

SUMMARY

I. Title

Numerical Modeling of Tombolo Formation

II. Significance and objectives of the study

Offshore breakwaters have been used as a means to protect beaches against severe erosion. The currents engendered behind the breakwaters by waves deposit sediments in the sheltered area to bulid a new morphological shape called a salient. Sometimes the salient grows until its apex reaches the breakwater to form a tombolo. There are few numerical models that can simulate the formation of tombolos. Most of the numerical models stop computation when the computed shoreline reaches the breakwater or predict outgrowth of the salient over the breakwater. In this study, a one-line numerical model is developed that is capable of handling the formation and growth (or decay) of tombolos in the lee of impermeable offshore breakwaters.

III. Contents and results of the study

A one-line numerical model has been widely used for predicting shoreline change in the vicinity of coastal structures. Most one-line models reported to date use the Cartesian coordinate system, one of the axes of which is taken to be approximately parallel to the shoreline. The longshore sediment transport and the shoreline movement are assumed to be parallel and perpendicular, respectively, to this axis. If the shoreline makes a large angle with this axis as on a tombolo behind an offshore breakwater, however, this assumption is severely violated. To overcome this circumstance, models using a curvilinear coordinates that follow the shoreline have been developed, under the assumption that any point on the shoreline moves perpendicular to the instantaneous shoreline and the longshore sediment transport is parallel to the local shoreline. The present model also uses this curvilinear coordinate system.

When the shoreline attaches an impermeable offshore breakwater, its offshore movement should stop there. But the numerical model that does not appreciate the presence of the breakwater may predict shoreline positions passed over the breakwater. At each time step, the present model examines if any point of the shoreline has passed over the breakwater and pulls it back to the location of the breakwater if any. Instead, the neighboring shoreline positions are re-calculated so as to satisfy the conservation of sediment.

The developed model is applied to the simulation of the shoreline response during the first nine months after the construction of the Chippokes State Park Breakwater, Virginia, USA.

Numerical Modeling of Tombolo Formation

By Kyung Duck Suh,[1] Associate Member, ASCE and C. Scott Hardaway, Jr.[2]

Abstract

A one-line numerical model for predicting shoreline change in the vicinity of offshore breakwaters is developed. The model uses curvilinear coordinates that follow the shoreline and is capable of handling the formation of tombolos as well as the growth of salients. The project of six segmented breakwaters at Chippokes State Park, Virginia is reported. The developed model is applied to the simulation of the shoreline change during the first nine months after construction of the Chippokes breakwaters.

1 Introduction

Numerical shoreline change models are valuable tools for assessing beach changes in the vicinity of coastal structures. Advanced knowledge of waves and currents, and their interaction and the resulting sediment transport, associated with the increased capacities of large computers and improved numerical modeling algorithms, has made it possible to apply such complex models as a multi-line model (Perlin and Dean 1985) or general 3-D topographical change models (Wang et al. 1975; Watanabe 1982) to numerical modeling of shoreline problems. Due to the relatively accurate prediction of the shoreline change with less computational effort, however, the one-line model has been widely used. The GENESIS model (Hanson and Kraus 1989) is one of the more sophisticated one-line models, though its public access is yet limited. In the present paper, a one-line numerical model is developed that simulates the shoreline change in the lee of offshore breakwaters.

Offshore breakwaters have been used as a means to protect beaches against severe erosion. The currents generated behind the breakwaters by waves deposit sediments in the sheltered area to build a new morphological shape called a salient. Sometimes the salient

[1]Senior Researcher, Ocean Engineering Laboratory, Korea Ocean Research & Development Institute, Ansan P.O. Box 29, Seoul 425-600, Korea; formerly Marine Scientist at Virginia Institute of Marine Science.
[2]Marine Scientist, Division of Geological and Benthic Oceanography, Virginia Institute of Marine Science, Gloucester Point, VA 23062, USA.

grows until its apex reaches the breakwater to form a tombolo. There are few numerical models that can simulate the formation of tombolos. Most of the numerical models stop computation when the computed shoreline reaches the breakwater or predict outgrowth of the salient over the breakwater. Perlin (1979) proposed a method for handling the formation of a tombolo, but none of the numerical examples in his paper simulates a situation where a tombolo has formed. The present model was developed to permit the formation and growth (or decay) of tombolos in the lee of impermeable offshore breakwaters. The method used for tombolo calculation copies that proposed by Hanson and Kraus (1985) as a way of constraining the shoreline for the case of a seawall, the inverse of the problem of a breakwater. The present model uses curvilinear coordinates that follow the shoreline, as done in LeBlond (1972), Uda (1983), Suh (1985), and Kobayashi and Dalrymple (1986).

The project of six segmented breakwaters at Chippokes State Park, Virginia reported in Hardaway et al. (1988) is summarized in this paper. The developed model is applied to the simulation of the shoreline response during the first nine months after construction of the Chippokes breakwaters.

2 Numerical Model

2.1 Shoreline change model

The curvilinear coordinate system used in the present model is shown in Fig. 1 along with some other notations. The symbol s is the coordinate following the shoreline whose positive direction points to the right when facing seaward. $(x_s,\ y_s)$ is the location of an arbitrary point on the curved shoreline in terms of the Cartesian coordinate system.

$$\vec{m} = \left(\frac{\partial x_s}{\partial s}, \frac{\partial y_s}{\partial s}\right) = (\cos\theta, \sin\theta) \tag{1}$$

is the unit tangential vector to the shoreline in the direction of increasing s,

$$\vec{n} = \left(-\frac{\partial y_s}{\partial s}, \frac{\partial x_s}{\partial s}\right) = (-\sin\theta, \cos\theta) \tag{2}$$

is the seaward unit normal vector to the shoreline, and θ is the angle between $\vec{m}$ and the x-axis which is measured counterclockwise from the positive x-direction. In the figure, Q is the volumetric longshore sediment transport rate and α_b is the breaking wave angle between the wave crest and the x-axis which is measured counterclockwise from the positive x-direction.

Assume that the point, (x_s, y_s), moves perpendicular to the shoreline, so that

$$\left(\frac{\partial x_s}{\partial t}, \frac{\partial y_s}{\partial t}\right) = e\vec{n}, \tag{3}$$

in which e is the rate of shore-normal movement of shoreline. Using the notation of complex variables,

$$z_s = x_s + iy_s, \tag{4}$$

in which $i = \sqrt{-1}$, and expressing e as

$$e = -\frac{1}{D}\frac{\partial Q}{\partial s}, \tag{5}$$

Eq. (3) can be written as

$$\frac{\partial z_s}{\partial t} = -\frac{1}{D}\frac{\partial Q}{\partial s}\exp\left\{i\left(\theta + \frac{\pi}{2}\right)\right\}, \tag{6}$$

in which D is the depth of profile closure at which no measurable change in bottom elevation occurs. If θ is very small, this equation reduces to the sediment continuity equation of traditional one-line models using the Cartesian coordinate system.

A widely-used expression for the longshore sediment transport rate in places where diffraction dominates is that proposed by Ozasa and Brampton (1980):

$$Q = \Gamma H_b^{5/2} \left\{ K_1 \sin(2\delta_b) - K_2 \frac{\partial H_b}{\partial s} \cot\beta \cos\delta_b \right\}, \tag{7}$$

in which

$$\Gamma = \frac{g^{1/2}}{16(s_s - 1)(1-p)\kappa^{1/2}}, \tag{8}$$

$$\delta_b = \alpha_b - \theta \tag{9}$$

is the breaking wave angle relative to the shoreline under the assumption that the breakerline and the shoreline are locally parallel, and g = gravitational acceleration; s_s = specific gravity of sediment relative to fluid; p = porosity of sediment; κ = ratio of wave height to water depth at breaking; H_b = breaking wave height; $\tan\beta$ = beach slope; K_1, K_2 = empirical longshore sediment transport coefficients. The first term in Eq. (7) describes the sediment transport rate due to obliquely incident waves, whereas the second term describes the transport due to longshore gradient of breaking wave heights, which has been found to be of great importance in cases where diffraction dominates. The beach slope is calculated by the empirical formula proposed by Sunamura (1984) for given breaking wave height, wave period and sand grain size.

A number of studies has been performed to determine the coefficient K_1. A value of $K_1 = 0.77$ was originally determined by Komar and Inman (1970), and a decrease from 0.77 to 0.58 was recommended by Kraus et al. (1982). The second transport coefficient, K_2, has not received great attention of researchers. Ozasa and Brampton (1980) used $K_2 = 3.24K_1$. Hanson and Kraus (1989), however, recommended that the value of K_2 is typically 0.5 to 1.0 times that of K_1.

One of the basic assumptions of one-line models is that the beach has a constant depth of profile closure throughout the model area, within which erosion or accretion of beach occurs. As done in Kraus and Harikai (1983), the expression proposed by Hallermeier (1983) is adopted with a deep water wave height, H_o, in place of the extreme wave height for an annual seaward limit of profile change:

$$D = \frac{2.9H_o}{(s_s - 1)^{1/2}}. \tag{10}$$

In the model, the greatest H_o during the simulation period is used for calculation of D.

2.2 Breaking wave model

The sediment continuity equation, (6), can be solved for the shoreline position, z_s, if the wave heights and angles along the breakerline are given. In the present model, the wave condition (height, period and angle of incidence) at the location of the breakwaters is given as input data and the wave deformation in the lee of the breakwaters is computed. It is assumed that the wave condition is constant along the line connecting the breakwaters and its longshore extensions to the lateral boundaries. This assumption will be appropriate if the offshore bottom topography does not deviate drastically from straight and parallel contours, the offshore distances of the breakwaters are almost constant, and the longshore distance of the model area is not too long.

The three major phenomena which alter the wave in the lee of the breakwaters are refraction, diffraction and shoaling. There are some means to compute the combined wave refraction-diffraction, e.g., Larsen (1976) or Southgate (1985), if the bathymetry between the breakwaters and the shoreline is known. But that is not the case for a one-line model. Thus, in the present model, it is assumed that all these wave phenomena occur independently, so that the breaking wave height, H_b, can be calculated by

$$H_b = K_D K_R K_S H_B, \tag{11}$$

in which H_B = wave height at the location of breakwaters, and K_D, K_R, K_S = coefficients of diffraction, refraction, and shoaling. The remainder of this section is devoted to the computation of these coefficients. The procedure for computing the breaking wave angle will be explained where appropriate.

For illustration, let us consider two offshore breakwaters as shown in Fig. 2. The shoreline on the left salient will be affected by both the wave diffracted around the left tip of the left breakwater and the wave diffracted through the gap. Perlin (1979) assumed that each wave behaves independently and the resulting sediment transport can be calculated by adding vectorially the sediment transported by each wave. Kraus (1983) used the highest wave of the two waves to calculate the sediment transport. The Kraus' approach adopted in this study looks more reasonable as the salient grows or a tombolo is formed. The entire shoreline shown in Fig. 2, then, can be devided into three diffraction regions affected by diffraction around the left tip of the left breakwater, through the gap, and around the right tip of the right breakwater, respectively.

The diffraction analysis used in this model is based on the theory of Penney and Price (1952). The assumptions in their theory include a semi-infinitely long breakwater with an infinitesimal thickness, linear theory and a constant depth. In the left diffraction region in Fig. 2, the breakwater is assumed to be infinitely long to the right direction and the constant water depth is taken as the depth at the breakwater tip. Similar assumptions are made for the right diffraction region. In the central diffraction region behind the gap, each breakwater is assumed to be infinitely long to the directions away from the gap, and the solutions from each breakwater are superimposed to calculate the actual diffraction coefficient in that region. The diffraction coefficient at the breakerline position, $B(x_b, y_b)$, in Fig. 2, is assumed to be the same as that calculated for the corresponding shoreline position, $S(x_s, y_s)$.

The method of determining the breaking wave angle closely follows that of Kraus (1982). First, for each point of the shoreline, the offshore bottom contours from the shoreline to the location of the breakwater tip are assumed to be straight and parallel to the local orientation of the shoreline. The approximate location of wave breaking, (x_b, y_b), corresponding to the shoreline position, (x_s, y_s), is calculated by

$$(x_b, y_b) = (x_s - w_b \sin\theta,\ y_s + w_b \cos\theta), \tag{12}$$

in which w_b is the surf zone width. For the breaking points located in Zone I, III, or V in Fig. 2, the breaking wave angle and the coefficients of refraction and shoaling can be computed by regular refraction/shoaling analysis on a beach with straight iso-baths.

In Zone II and IV in Fig. 2, the diffracted wave crests near the tips of the breakwaters are assumed to be circular in planform. The diffracted wave is then refracted shoreward. Fig. 3 is the enlargement of the left half of Fig. 2. The wave reached at the left tip of the breakwater with an angle α_B is diffracted and leaves the tip with an angle θ_R to refract to the breaking point, B_1. The unknown angle, θ_R, is measured counterclockwise from the line which is perpendicular to the assumed straight and parallel bottom contours. It is convenient to use the local shoreline-oriented coordinates (x', y') as shown in Fig. 3, which are related to the computational coordinates (x, y) by

$$(x', y') = ((x - x_b)\cos\theta + (y - y_b)\sin\theta,\ -(x - x_b)\sin\theta + (y - y_b)\cos\theta)\,. \tag{13}$$

The origin $(x', y') = (0, 0)$ corresponds to the breaking point $B_1(x_b, y_b)$. Following the procedure given in Kraus (1982), an equation for θ_R can be obtained as

$$x'_l = \frac{y'_l}{\sin^2\theta_R}\left\{\sin\theta_R\cos\theta_R + \sin^{-1}(\cos\theta_R) - \sin^{-1}(1)\right\}, \tag{14}$$

in which (x'_l, y'_l) is the location of the left tip of the breakwater in terms of the shoreline-oriented coordinates (x', y'). The above equation can be used with (x'_r, y'_r) instead of (x'_l, y'_l) when the wave is diffracted around the right tip of the breakwater. In this case, θ_R and the shoreline-oriented coordinates (x', y') are redefined as shown in Fig. 3.

Eq. (14) can be solved for θ_R by the Newton-Raphson method. The breaking wave angle, α'_b, relative to the x'-axis is calculated by Snell's law:

$$k_B \sin\theta_R = k_b \sin\alpha'_b, \tag{15}$$

and the breaking angle, α_b, relative to the x-axis is then given by

$$\alpha_b = \begin{cases} \alpha'_b + \theta & \text{for waves diffracted at the left tip,} \\ -\alpha'_b + \theta & \text{for waves diffracted at the right tip.} \end{cases} \tag{16}$$

The corresponding refraction and shoaling coefficients are computed by

$$K_R = \left(\frac{\cos\theta_R}{\cos\alpha'_b}\right)^{1/2}, \qquad K_S = \left(\frac{C_{g_B}}{C_{g_b}}\right)^{1/2}, \tag{17}$$

in which the subscripts B and b refer to the values at the location of breakwater and wave breaking, respectively. As the salient grows, in the region near the apex of the salient, θ_R bigger than $\theta_{R_{max}}$ can be calculated, but this is impossible due to the presence of the breakwater. The breaking wave angles in this region are obtained by the interpolation (proportional to the longshore distance) from those at the ends of that region, and the refraction coefficients are assumed to be 1.0.

2.3 Finite-difference equations and boundary conditions

An explicit finite-difference method is used to solve Eqs. (6), (7) and (9) numerically for the wave condition computed along the shoreline. The location and orientation of the shoreline and the breaking wave angle are defined at the nodal points, and the longshore transport rate is defined between the nodal points, as shown in Fig. 4. The sediment continuity equation, (6), at the ith point can be expressed as the following finite-difference form:

$$z'_{s_i} = z_{s_i} + \frac{\Delta t}{D}\left(\frac{Q_{i-1} - Q_i}{\frac{1}{2}(\Delta s_i + \Delta s_{i-1})}\right)\exp\left\{i\left(\frac{\theta_i + \theta_{i-1}}{2} + \frac{\pi}{2}\right)\right\}, \tag{18}$$

in which Δt is the time step. The prime denotes the quantity being solved for the next time step and the unprimed quantities are known quantities at the present time step. The quantities, Δs_i, θ_i, and Q_i, are computed by

$$\Delta s_i = \left\{(x_{s_{i+1}} - x_{s_i})^2 + (y_{s_{i+1}} - y_{s_i})^2\right\}^{1/2}, \tag{19}$$

$$\theta_i = \tan^{-1}\left(\frac{y_{s_{i+1}} - y_{s_i}}{x_{s_{i+1}} - x_{s_i}}\right), \tag{20}$$

and

$$Q_i = \Gamma\left(\frac{H_{b_i} + H_{b_{i+1}}}{2}\right)^{5/2}\left\{K_1 \sin(2\delta_{b_i}) - K_2 \frac{H_{b_{i+1}} - H_{b_i}}{\Delta s_i}\left(\frac{\cot\beta_i + \cot\beta_{i+1}}{2}\right)\cos\delta_{b_i}\right\}, \tag{21}$$

in which

$$\delta_{b_i} = \frac{\alpha_{b_i} + \alpha_{b_{i+1}}}{2} - \theta_i. \tag{22}$$

The explicit finite-difference scheme gives unstable solution for a large time step Δt. As done in Kraus and Harikai (1983), an approximate stability criterion for small δ_b can be obtained as

$$\Delta t \leq \frac{1}{2}\frac{(\Delta x_s)^2}{\epsilon}, \tag{23}$$

in which $\epsilon = 2K_1\Gamma H_b^{5/2}/D$. This stability criterion can give the first approximation of the time step for stable solution. If the computed shoreline shows saw-tooth instability, a smaller time step will be needed. Such an instability can be suppressed by smoothing shoreline orientation, longshore transport rate, and shoreline position as done in Uda (1983), but the smoothing process of shoreline position introduces an error in the conservation of sand as Δx increases.

There may be several types of boundary conditions implemented depending on the situation at the extremeties of the shoreline stretch to be modeled. The first is a fixed beach at the boundaries, which implies that the sediment transport rate remains constant near the boundaries so that the beach retains an equilibrium state there. The fixed boundary condition is applicable when the length of the beach is large enough so that the sediment transport at the boundaries does not affect the region where the offshore breakwaters are

simulated. The second is a floating boundary condition which allows the shoreline to change at the boundaries by assuming linear variation of longshore sediment transport rate near the boundaries, for example, $Q_{IB+1} = 2Q_{IB} - Q_{IB-1}$, in which IB indicates model boundary. The third is a no-flux boundary condition which is applicable in the case in which there is an impermeable terminal groin at the boundary. The last one is a forced boundary condition, which is applicable when the movement of the boundary is *a priori* known. In the present model, if the forced boundary condition is used the final position of the boundary is given as input data and it is assumed that the shoreline at the boundary moves in proportion to the elapsed time from the initial position to the final position.

2.4 Treatment of tombolo formation

When the shoreline attaches an impermeable offshore breakwater, its offshore movement should stop there. But the numerical model that does not appreciate the presence of the breakwater may predict shoreline positions moved seaward of the breakwater. Thus, at each time step the predicted shoreline position should be examined to determine if any point has moved seaward of the breakwater. If so, it should be pulled back to the location of the breakwater. Hanson and Kraus (1985) proposed a method to incorporate seawall constraint in a one-line numerical model. The method permits a grid point to move landward of the position of a seawall in the initial computation, and then adjusts the longshore transport rates near that point so as to pull it back to the location of the seawall. In the present paper the same method is used for the case of an offshore breakwater.

Consider the discretized shoreline position as shown in Fig. 5. The dashed line denotes the shoreline position at the previous time step, and the solid line and dash-dotted line denote the uncorrected and corrected shoreline positions, respectively, at the present time step. In the following analysis, the primed quantities represent the uncorrected shoreline position. In Fig. 5, the ith point moved seaward of the breakwater to reach the point $C'(x'_{s_i}, y'_{s_i})$. We want to pull it back to the point $C(x_{s_i}, y_{s_i})$, which is the intersection of

the breakwater and the line passing the points C and C'. The equation of the breakwater whose tips are located at (x_l, y_l) and (x_r, y_r) is

$$y = (x - x_l)\tan\theta_B + y_l, \tag{24}$$

in which θ_B is the angle between the breakwater and the x-axis which is measured counter-clockwise from the positive x-direction. The equation of the line passing the points C and C' is

$$y = (x'_{s_i} - x)\cot\frac{\theta_{i-1} + \theta_i}{2} + y'_{s_i}, \tag{25}$$

in which θ_i and θ_{i-1} are as defined in Fig. 4, and $-\cot\{(\theta_{i-1} + \theta_i)/2\}$ represents the slope of the line passing the points C and C'. The location of the point C is then calculated as the intersection of the lines expressed by Eqs. (24) and (25).

As done in Hanson and Kraus (1985), the fictitious transport rate of sand, ΔQ_{fic}, contributed to move the shoreline position from C' to C can be calculated by putting z_{s_i} for the point C and z'_{s_i} for the point C' in Eq. (18) as

$$\Delta Q_{fic} = \frac{D(\Delta s_i + \Delta s_{i-1})}{2\Delta t}\exp\left\{-i\left(\frac{\theta_i + \theta_{i-1}}{2} - \frac{\pi}{2}\right)\right\}(z'_{s_i} - z_{s_i}). \tag{26}$$

The amount ΔQ_{fic} must be subtracted from the computed transport rates (Q_{i-1} and/or Q_i) depending on their directions as follows:

$$\left.\begin{aligned} Q^c_{i-1} &= Q_{i-1} - \Delta Q_{fic}\frac{Q_{i-1}}{Q_{i-1} - Q_i} \\ Q^c_i &= Q_i - \Delta Q_{fic}\frac{Q_i}{Q_{i-1} - Q_i} \end{aligned}\right\} \quad \text{if} \quad Q_{i-1} \geq 0 \text{ and } Q_i \leq 0, \tag{27}$$

$$Q^c_{i-1} = Q_{i-1} - \Delta Q_{fic} \quad \text{if} \quad Q_{i-1} \geq 0 \text{ and } Q_i > 0, \tag{28}$$

$$Q^c_i = Q_i + \Delta Q_{fic} \quad \text{if} \quad Q_{i-1} < 0 \text{ and } Q_i \leq 0. \tag{29}$$

The superscript c denotes the corrected transport rates. The new position of the point B and/or D is then calculated using the corrected transport rates. If the new point, B or D, is computed to move seaward of the breakwater, it is pulled back to the location of the

breakwater using the same procedure as above. Finally, it should be mentioned that in the present model, if any two adjacent shoreline points touch the breakwater, the transport rate between these points is set to zero.

3 Chippokes State Park Breakwater Project

The six segmented breakwaters at Chippokes State Park is located on the southern shore of Cobham Bay in James River, one of the tributary estuaries of Chesapeake Bay, Virginia (Fig. 6). Chippokes is a recreational and historic state park as well as a model farm. The site is characterized by high (12 m) eroding fastland banks composed of a lower unit of shelly, fossiliferous, fine to coarse sand overlain by an upper layer of slightly muddy, fine to medium sand.

The preconstruction beach at Chippokes was a curvilinear strand of sand about 7.5 m wide from MHW to the base of the bank. The beach itself consists of well sorted, shelly sand derived from the eroding bluff. The mean diameter of the beach sand averaged from six sediment samples is 0.44 mm (medium sand). The shoreline at Chippokes fasces almost due north and has an average fetch of about 4.8 km. Long fetch exposures of 9.3 km and 14.8 km occur to NNE and NW directions, respectively. Net longshore transport here is eastward but with seasonal fluctuations and on-offshore movement. The seasonal wave climate favors northerly winds in winter and southwesterly winds in summer. Mean seasonal winds generate limited waves across the river. Extratropical and tropical storms with the associated storm surges are the main forces causing movement of beach sand and shoreline erosion. Mean tidal range is 58 cm.

The goal of the project was to design a system which would permit tombolos to form utilizing the existing volume of sand on the beach such that with time a stable backshore would develop and protect the base of the high banks. A system of six breakwater units with a length to gap ratio of 1:1.5 was designed. The crest lengths are 15 m and gaps are

22.5 m. The centerline of the breakwaters is approximately 9 m from the initial MHW line. The water depth below MHW at the location of breakwaters varies between 0.75 and 0.87 m. Construction of the six rubble mound breakwaters took place during June 1987.

The baseline (x-axis in Fig. 7) was established using a transit. From this, 33 profile lines were determined and surveys performed using a rod and level. Profile measurements were made in July 28 and November 12, 1987 and February 23, 1988. Aerial photography was done every three months between September 2, 1987 and March 9, 1988. The photographs were used along with the profile data to create the shoreline map.

Fig. 7 shows the measured shoreline change (dashed lines) from June 1987 to March 1988 along with the computed results. The position of MHW was used to track beach changes. Sand began accumulating and migrating toward each breakwater unit as cuspate spits formed almost immediately after construction. The characteristic double salients evolved behind each breakwater by September 1987. Sediment for the salients was derived from the adjacent embayments. By March 1988 all the bays showed signs of filling. Especially obvious are the accumulation of sand on the west end of the system and marked loss of sand on the east. One would infer a net west to east movement of sand along this portion of the reach.

4 Application

The developed numerical model was applied to the simulation of the shoreline change near the Chippokes State Park Breakwaters for the first nine months (from June 1987 to March 1988) after construction.

4.1 Wave hindcast

There are no available wave data near the project site for the simulation period. Therefore, input wave data at the location of the breakwaters were hindcasted from wind data at

Hog Island, Surry County, Virginia (see Fig. 6). For the periods of missing data (several times of a few days), the wind data at Norfolk, Virginia (located about 50 km southeast of the project site) were used. The wind data included speed and direction every one hour. Assuming that the wave direction corresponds to the wind direction, as seen in Fig. 6, the project site is affected by the wind blowing within the directional window fanning from 320^o to 20^o measured clockwise from true north. It is also assumed that in order to generate the wave field that affects the shoreline change, wind should blow for more than three hours (i.e., more than three consecutive observations) within the directional window. The average wind speed and direction for the period were calculated by vector-averaging the observations given every one hour. A constant wind field corresponding to the averaged wind speed and direction was assumed for that period.

The significant wave height and period at the location of the breakwaters were computed using the method of Kiley (1989), which is essentially a shallow water estuarine version of the quasi-empirical wind wave prediction model developed by Bretschneider (1966) and modified by Camfield (1977). The method includes variation in water depth, the effect of surrounding land forms on the computation of the effective fetch, wave growth due to wind stress and wave decay due to bottom friction and percolation. The wave angle at the location of the breakwaters is determined by Snell's law assuming that the offshore bottom contours are straight and parallel to the x-axis and the deep water wave direction (at the center of the river) is same as the wind direction.

The weight-averaged (by duration of each wave condition) values of significant wave height and period, and wave angle at the location of breakwaters are 12.2 cm, 1.43 sec, and 1.33^o, respectively, indicating very short small waves and net eastward longshore transport rate. Total duration of the simulation is 568 hours so that the percent of calm is 90 %.

4.2 Simulation

The initial shoreline in June 1987 in Fig. 7 was discretized by $\Delta x = 1.524\ m$ (5 ft) to give about 10 points behind each breakwater and 195 points (296 m) for the shoreline reach shown in Fig. 7. $\Delta t = 90\ sec$ was used. All the water depths and shoreline position in the model are with respect to MHW level, since the shoreline position in the report of Hardaway et al. (1988) is presented in terms of MHW line. The water level was assumed to be fixed at the MHW level. The coordinates of the breakwater tips were taken as the shoreward corners of the bases of the breakwaters.

The shoreline change in the areas far from the project site is not available. Therefore, the model area was extended to both sides by 100 m and fixed boundary conditions were used at both ends. The offshore distances of the initial shoreline in the extended areas were assumed to be the same as those at the end points of the initial shoreline in Fig. 7. The shoreline change in the extended areas is not shown in Fig. 7.

The longshore sediment transport coefficient $K_1 = 0.77$ was used as suggested by Komar and Inman (1970). $K_2 = K_1$ was used tentatively. The calculated depth of profile closure is 0.52 m.

Fig. 7 shows the computed (solid lines) shoreline changes in September 2, 1987 and March 9, 1988 along with the measurement (short-dashed lines). The initial shoreline position is also given by long-dashed lines. The formation of double salients in September 1987 is predicted by the model, even though it is not so clear as in the measurement. The model calculated smaller tombolos and more prominent erosion behind the gaps compared to those in the measurement in March 1988. This may be due to the addition of sediment to the system by runoff and bank erosion as reported in Hardaway et al. (1988), which was not included in the present model that assumes zero on-offshore transport of sediment.

4.3 Sensitivity tests

There are no other coastal structures or geographical features that directly affect the beach at the Chippokes project site, and the shoreline change in the areas far from the breakwaters is not available. Therefore, the choice of boundary condition is arbitrary and sensitivity of the calculated shoreline response to different boundary conditions should be examined.

Fig. 8 shows the shoreline positions calculated with various boundary conditions along with the measured shoreline in March 9, 1988. The shoreline position in the embayments does not show any difference for different boundary conditions. The extension of the model boundaries (by 50 m to both sides) gives little difference (see open circles and solid line in Fig. 8). The floating boundary condition slightly increases updrift accretion and downdrift erosion, giving better agreement with the measurement than the fixed boundary condition. As it should do, the forced boundary condition gives the best results.

Fig. 9 shows the calculated shoreline positions for different values of the longshore transport coefficients K_1 and K_2 and the depth of closure D. The calculated shorelines with a smaller value of K_1 or K_2 than 0.77 are almost identical to that calculated with $K_1 = K_2 = 0.77$. Calculation using $D = 1.0\ m$, almost twice the value used in the previous simulations, reduces the accretion behind the breakwaters and erosion in the embayments as expected by Eq. (6).

4.4 Decay of tombolos

Sometimes tombolos are built artificially as a means to protect beaches as in Elm's Beach, Maryland (Hardaway and Gunn 1989), for example. If the project is not designed properly, the tombolos can be reduced to salients. In order to test how the model works for such a situation, the model was run for 48 hours of $H_B = 7.9\ cm$, $T = 1.16\ sec$, and $\alpha_B = 0^o$ (the mildest wave condition used in the previous simulation) with the computed shoreline in March 9, 1988 as the initial condition. The result is shown in Fig. 10. For the mild wave

condition, the tombolos reduced to salients and accretion occurred in the embayments.

5 Conclusion

A one-line numerical model for predicting shoreline change in the vicinity of offshore breakwaters has been developed and compared with the field data at Chippokes State Park Breakwaters, Virginia. The model is capable of handling the growth and decay of tombolos as well as salients.

The present model that assumes zero on-offshore transport of sediment predicted smaller tombolos and more embayment erosion compared to those in the measurement at the Chippokes project site, where sediment was added to the system by runoff and bank erosion.

The calculated shoreline response in the embayments between the breakwaters is not affected by the choice of boundary condition. But the magnitude of updrift accretion and downdrift erosion shows significant change depending on the boundary condition applied. The calculated shoreline response was not so sensitive to the change of the longshore transport coefficients K_1 and K_2. Doubling the depth of profile closure D reduced the accretion behind the breakwaters and erosion in the embayments.

Acknowledgements

This study was partly supported by Korea Ocean Research and Development Institute under Grant No. PE-00223.

Appendix. References

1. Bretschneider, C.L. (1966). "Wave generation by wind, Deep and shallow water." In: *Estuary and Coastline Hydrodynamics* (Ed. A.T. Ippen). McGraw-Hill, New York, 133-196.

2. Camfield, F.E. (1977). "A method for estimating wind-wave growth and decay in shallow water with high values of bottom friction." *Tech. Aid CETA 77-6.* Coast. Engrg. Res. Center, Fort Belvoir, Virginia.

3. Hallermeier, R.J. (1983). "Sand transport limits in coastal structure design." *Proc. Coast. Structures '83*, ASCE, 703-716.

4. Hanson, H. and Kraus, N.C. (1985). "Seawall constraint in shoreline numerical model." *J. Wtrwy., Port, Coast. and Oc. Engrg.* 111(6), 1079-1083.

5. Hanson, H. and Kraus, N.C. (1989). "GENESIS: Generalized model for simulating shoreline change; Report 1, Technical Reference." *Tech. Rep. CERC-89-19.* Coast. Engrg. Res. Center, Waterways Experiment Station, Vicksburg, Miss.

6. Hardaway, C.S. and Gunn, J.R. (1989). "Elm's Beach breakwater project – St. Mary's County, Maryland."

7. Hardaway, C.S., Thomas, G.R., Moustafa, M.S.J. and Li, J.-H. (1988). "Chesapeake Bay Shoreline Study - Interim Report." Virginia Inst. of Marine Sci., Gloucester Point, Virginia.

8. Kiley, K. (1989). "Estimates of bottom water velocities associated with gale wind generated waves in the James River, Virginia." *Unpublished manuscript.* Virginia

Inst. of Marine Sci., Gloucester Point, Virginia.

9. Kobayashi, N. and Dalrymple, R.A. (1986). "Erosion of unprotected causeway due to waves." *Res. Rep. No. CE-86-58.* Dept. of Civil Engrg., Univ. of Delaware, Newark, Del.

10. Komar, P.D. and Inman, D.L. (1970). "Longshore sand transport on beaches". *J. Geophys. Res.* 75(30), 5914-5927.

11. Kraus, N.C. (1982). "Pragmatic calculation of the breaking wave height and wave angle behind structures." *Proc. 29th Japanese Coast. Engrg. Conf.*, 95-99 (in Japanese).

12. Kraus, N.C. (1983). "Application of a shoreline prediction model." *Proc. Coast. Structures '83*, ASCE, 632-645.

13. Kraus, N.C. and Harikai, S. (1983). "Numerical model of the shoreline change at Oarai beach." *Coast. Engrg.* 7, 1-28.

14. Kraus, N.C., Isobe, M., Igarashi, H., Sasaki, T. and Horikawa, K. (1982). "Field experiments on longshore sand transport in the surf zone." *Proc. 18th Coast. Engrg. Conf.*, ASCE, 969-988.

15. Larsen, J. (1978). "A harbour theory for wind-generated waves based on ray methods." *J. Fluid Mech.* 87, 143-158.

16. LeBlond, P.H. (1972). "On the formation of spiral beaches." *Proc. 13th Coast. Engrg. Conf.*, ASCE, 1331-1345.

17. Ozasa, H. and Brampton, A.H. (1980). "Mathematical modelling of beaches backed by seawalls." *Coast. Engrg.* 4(1), 47-63.

18. Penney, W.G. and Price, A.T. (1952). "The diffraction theory of sea waves and the shelter afforded by breakwaters." *Phil. Trans. Roy. Soc. London.* A 244, 236-253.

19. Perlin, M. (1979). "Predicting beach planforms in the lee of a breakwater." *Proc. Coast. Structures '79*, ASCE, 792-808.

20. Perlin, M. and Dean, R.G. (1985). "3-D model of bathymetric response to structures." *J. Wtrwy., Port, Coast. and Oc. Engrg.* 111(2), 153-170.

21. Southgate, H.N. (1985). "A harbor ray model of wave refraction-diffraction." *J. Wtrwy., Port, Coast. and Oc. Engrg.* 111(1), 29-44.

22. Suh, K.D. (1985). "Modeling of beach erosion control measures in a spiral wave basin", thesis submitted to the Univ. of Delaware, Newark, Del., in partial fulfillment of the requirements for the degree of Master of Civil Engineering.

23. Sunamura, T. (1984). "Quantitative predictions of beach-face slopes." *Geological Soc. of America Bull.* 95, 242-245.

24. Uda, T. (1983). "Predictive model of planform change of a spit at a river mouth." *Coast. Engrg. in Japan*, 26, 137-150.

25. Wang, H., Dalrymple, R.A. and Shiau, J.C. (1975). "Computer simulation of beach erosion and profile modification due to waves." *Proc. Symp. Modeling Technique*, ASCE. 1369-1384.

26. Watanabe, A. (1982). "Numerical models of nearshore currents and beach deformation." *Coast. Engrg. in Japan*, 25, 147-161.

Captions of figures

1. Curvilinear coordinate system and definition of model variables.
2. Zoning for computation of breaking wave angle and the coefficients of refraction and shoaling.
3. Refraction of the wave diffracted at the breakwater tip.
4. Finite-difference representation of shoreline and associated transport around ith point.
5. Illustration for tombolo calculation.
6. Location map of Chippokes State Park Breakwaters, Virginia.
7. Comparison between measurement and computation of shoreline change near Chippokes State Park Breakwaters, Virginia; (a) September 1987, (b) March 1988.
8. Model sensitivity to different boundary conditions.
9. Model sensitivity to changes in K_1, K_2 and D.
10. Test for decay of tombolos.

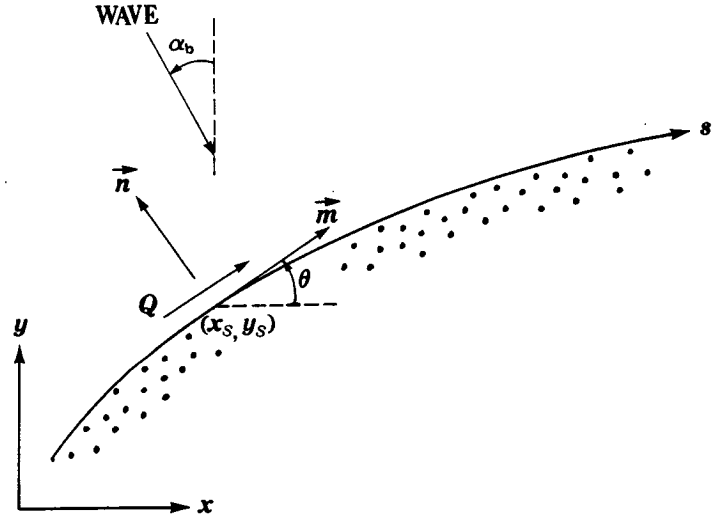

Fig. 1

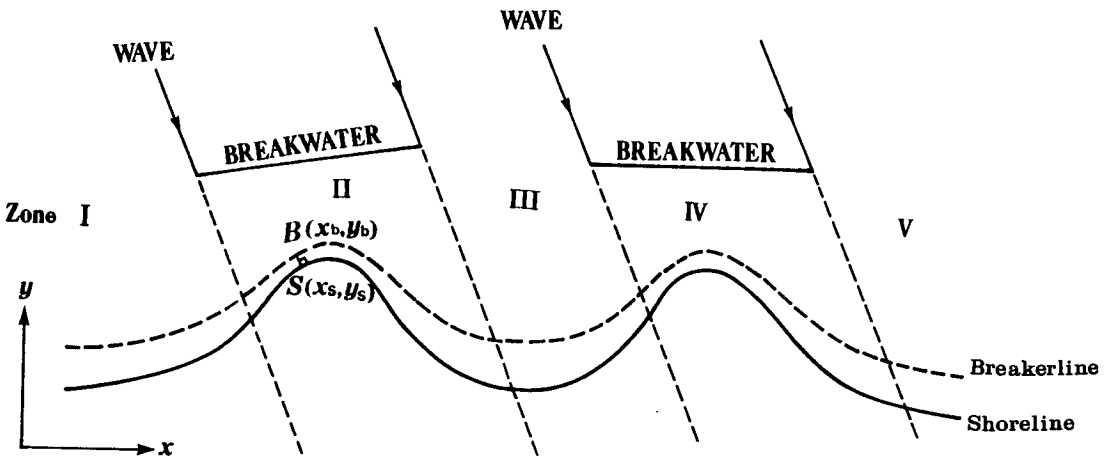
WAVE
WAVE
BREAKWATER
BREAKWATER
Zone I
II
III
IV
V
B(xb,yb)
S(xs,ys)
y
x
Breakerline
Shoreline

Fig. 2

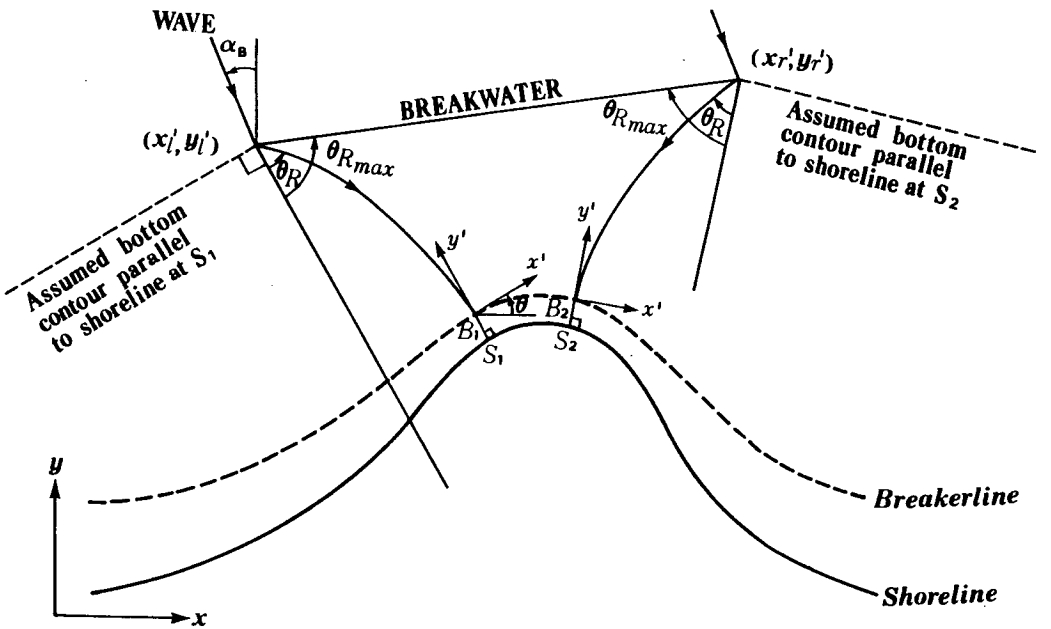
WAVE
α_B
BREAKWATER
(x_l', y_l')
(x_r', y_r')
$\theta_{R_{max}}$
θ_R
Assumed bottom contour parallel to shoreline at S_1
Assumed bottom contour parallel to shoreline at S_2
y'
x'
θ
B_1
B_2
S_1
S_2
y
x
Breakerline
Shoreline

Fig. 3

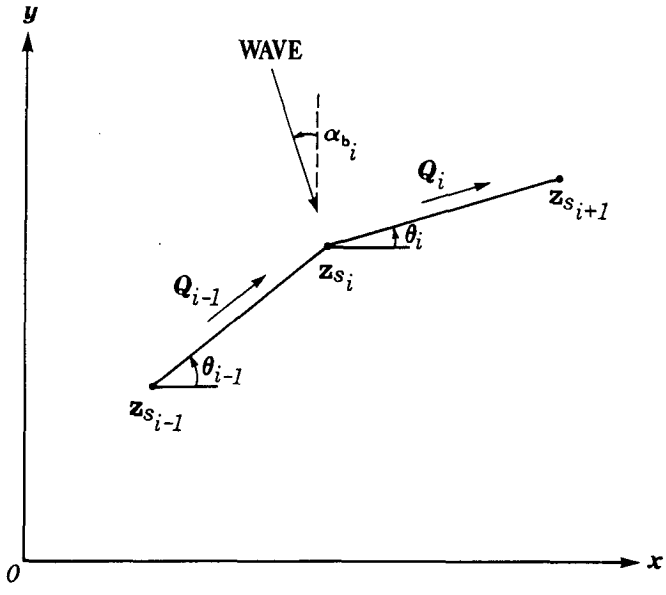

Fig. 4

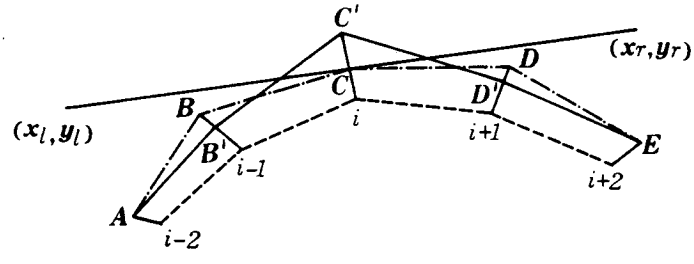

Fig. 5

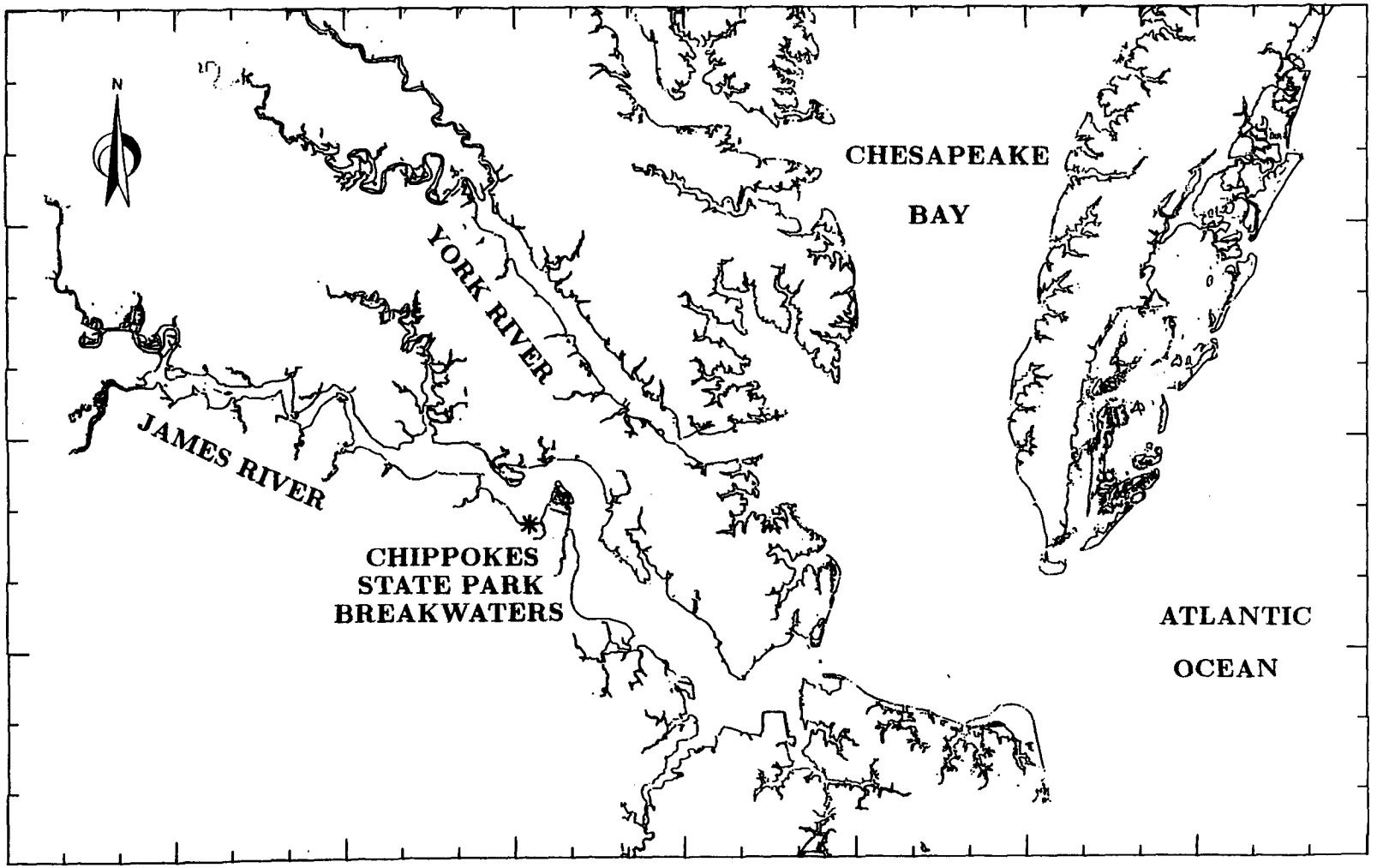
N
YORK RIVER
CHESAPEAKE
BAY
JAMES RIVER
CHIPPOKES
STATE PARK
BREAKWATERS
ATLANTIC
OCEAN

Fig. 6

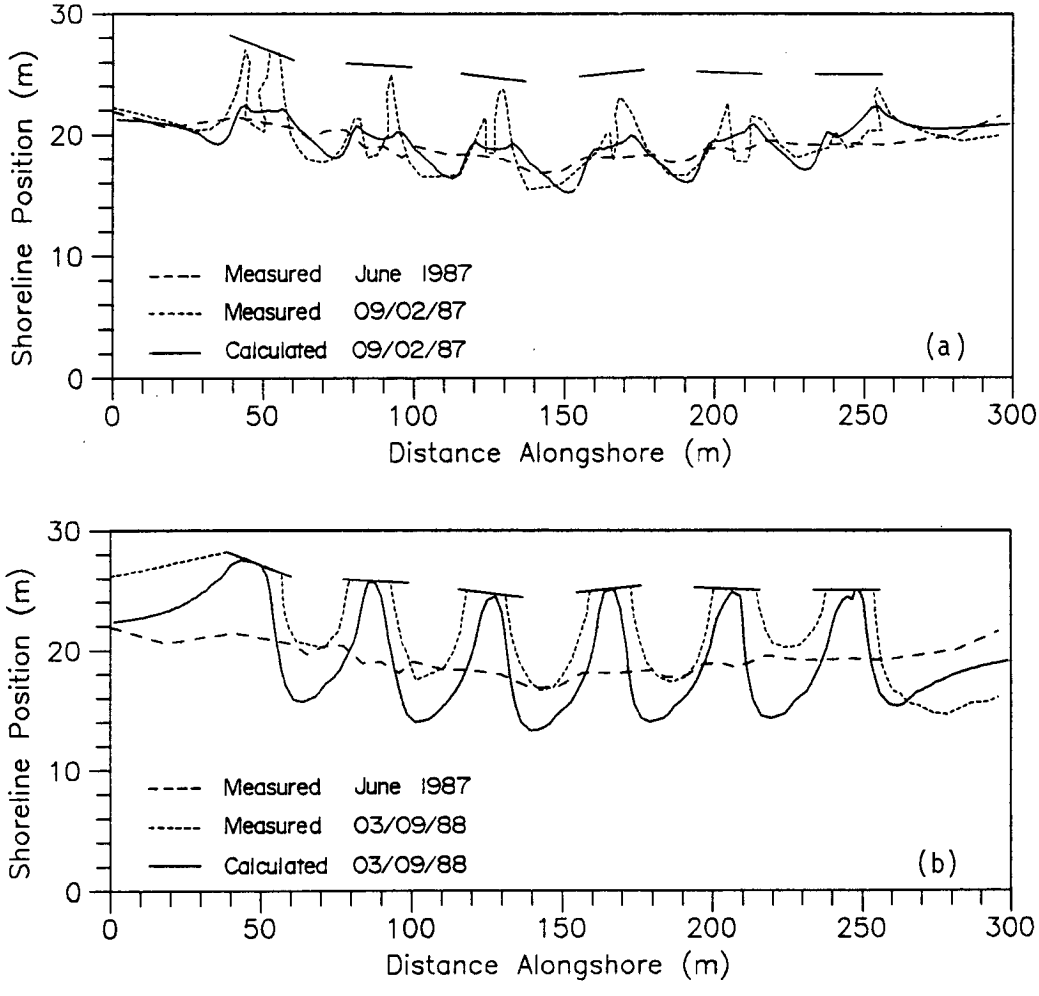
Shoreline Position (m)
30
20
10
0
0
50
100
150
200
250
300
Distance Alongshore (m)
Measured June 1987
Measured 09/02/87
Calculated 09/02/87
(a)
Shoreline Position (m)
30
20
10
0
0
50
100
150
200
250
300
Distance Alongshore (m)
Measured June 1987
Measured 03/09/88
Calculated 03/09/88
(b)

Fig. 7

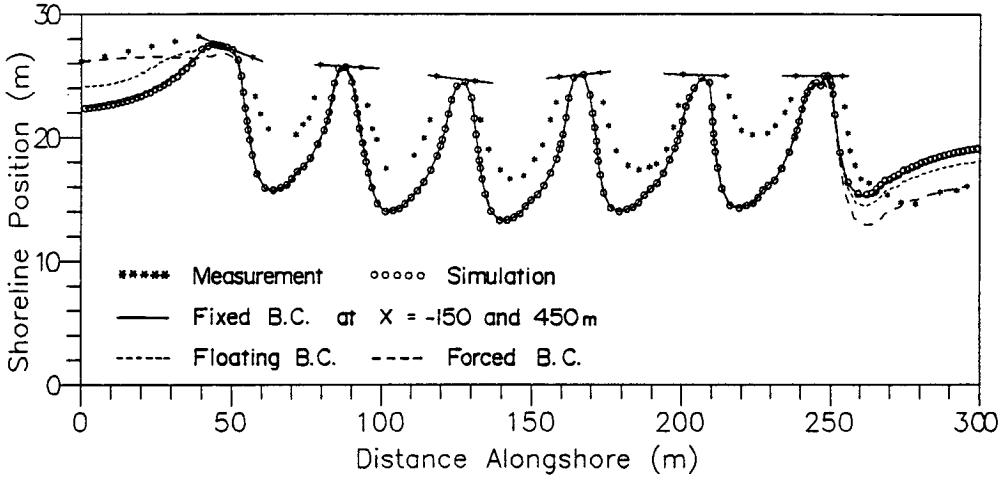
Shoreline Position (m)
30
20
10
0
0
50
100
150
200
250
300
Distance Alongshore (m)
***** Measurement
ooooo Simulation
Fixed B.C. at X = -150 and 450m
Floating B.C.
Forced B.C.

Fig. 8

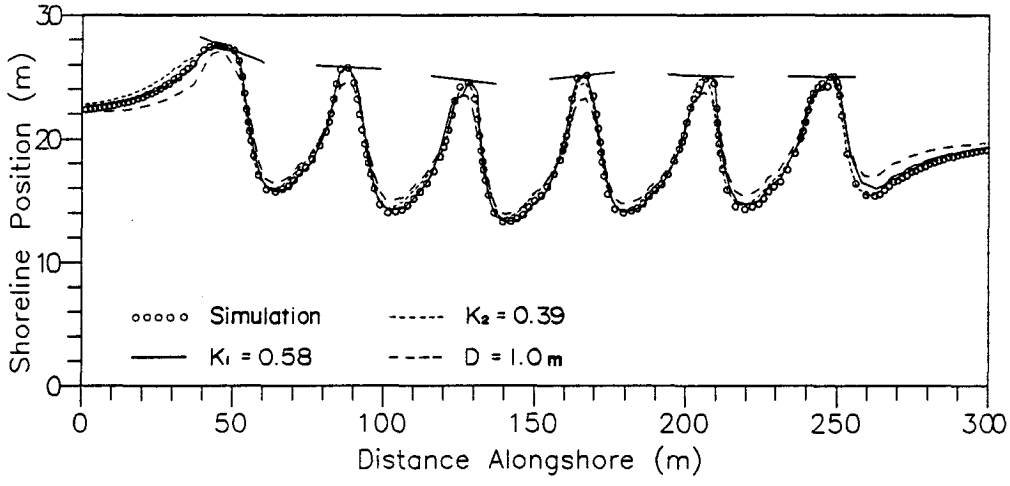
Shoreline Position (m)
30
20
10
0
0
50
100
150
200
250
300
Distance Alongshore (m)
ooooo Simulation
K₁ = 0.58
------ K₂ = 0.39
---- D = 1.0 m

Fig. 9